Modulation of circularly polarized luminescence by swelling of microgels functionalized with enantiopure [Ru(bpy) 3] 2+ luminophores

Kyohei Yoshida, Maino Kajiwara, Yutaka Okazaki, Lapeyre Véronique, Francesco Zinna, Neso Sojic, Laurent Bouffier, Jérôme Lacour, Valérie Ravaine, Reiko Oda

COMMUNICATION

Modulation of circularly polarized luminescence by swelling of microgels functionalized with enantiopure $[Ru(bpy)_3]^{2+}$ luminophores

eReceived 00th January 20xx,
Accepted 00th January 20xx

DOI: 10.1039/x0xx00000x

Kyohei Yoshida,[a,g] Maino Kajiwara,[b] Yutaka Okazaki,[c] Lapeyre Véronique,[d] Francesco Zinna,[e,f] Neso Sojic,[d] Laurent Bouffier,[d] Jérôme Lacour,[e] Valérie Ravaine*[d] and Reiko Oda*[a,h]

Abstract: Chemoresponsive microgels functionalised with enantiomeric Δ- or Λ- $[Ru(bpy)_3]^{2+}$ showed tunable chiroptical properties upon swelling and shrinking. The tuning of the absolute values and the ratio between the excitation and emission dissymmetry factors, g_{lum} and g_{abs}, is triggered by a modulation of the local mobility of $[Ru(bpy)_3]^{2+}$. This is done *via* addition of fructose, which controlled interactions and distances between $[Ru(bpy)_3]^{2+}$ and its enhancer, phenylboronic acid. Highest *g* values are observed for collapsed microgels in which phenylboronic acid and $[Ru(bpy)_3]^{2+}$ complexes have the strongest interactions.

Light polarization is a parameter crucial to control light-matter interactions. Among which, circular polarization is particularly attractive due to its angular independence. Recently, the possibility to tune circularly polarized luminescence (CPL) led to promising applications such as 3D displays through circularly polarized OLEDs[1-5], optical computer technologies[6], chemical or biological sensors[7-9], optical emissive devices[10], information system and security device[11]. Chiroptical properties of chiral emissive molecules[12-15], chiral or achiral supramolecular structures[16] in interaction with chiral templates of binary systems to generate CPL are well documented[10,17,18]. Switching the CPL response is challenging as it is difficult to instantaneously control the chemical structure of the luminophore or the chiral template for CPL generation. To date, it can be achieved by the introduction of additives such as salts (NaCl)[19] or ion pairs made of mono- and divalent cations[20], acid and base[21] in the CPL generation system, or the control of the molecular environment using solvent[22], UV-Vis irradiation[23], temperature[24,25], pH[25] or friction[26].

Here, we report a CPL modulation system based on the swelling/shrinking mechanism of a luminescent microgel functionalised with enantioenriched (4-vinyl-4-methyl-2,2'-bipyridine)bis(2,2-bipyridine)ruthenium(II) complex, simply denominated as $[Ru(bpy)_3]^{2+}$ in the following paragraphs (Fig. 1(a)). The soft matrix, made of a weakly cross-linked network, undergoes swelling upon addition of fructose, that acts as a stimulus decreasing the interaction between the luminophore and an enhancer, a phenylboronic acid (PBA) group in this case. Recently, Denisov et al.[27] synthesized poly(*N*-isopropylacrylamide) (pNIPAM) microgels functionalized by PBA and racemic $[Ru(bpy)_3]^{2+}$. In that study, it was shown that various stimuli could control the hydrogel swelling degree, including temperature and the presence/absence of monosaccharides. The diol groups of the sugar moieties could reversibly bind to the PBA groups to afford cyclic boronate esters.[27,28] Fructose displayed the highest binding constant and the strongest effect on swelling among the various monosaccharides tested.[29] The swelling/shrinking transition triggered the modification of the distance between the PBA and $[Ru(bpy)_3]^{2+}$ grafted moieties, therefore modulating their π–π and hydrophobic interactions. Photoluminescence (PL) properties (PL lifetime, quantum yield and PL peak wavelength) were hence influenced due to the molecular vibration control of the luminophore.[27] Herein, in a new development, we report the synthesis of the microgels with enantiopure $[Ru(bpy)_3]^{2+}$-based luminophores (R1: Δ, R2: Λ), (right- and left- handed propeller configurations respectively). We show that not only PL lifetime but also chiroptical properties such as g_{abs} and g_{lum} dissymmetry factors can directly be tuned by the swelling state and microenvironment variation of the microgels upon saccharide addition. To the best of our knowledge, such mechanisms have never been reported for the modulation of chiroptical signals. Microgel sample preparation procedure, chiral resolution of $[Ru(bpy)_3]^{2+}$ [31], as well as the characterisation are reported in the ESI and references therein. The molar ratio of PBA and $[Ru(bpy)_3]^{2+}$ in the microgel was chosen as 50 so that it ought to give the highest PL intensity.[27] First, the chemical structure and swelling/shrinking ability of the microgels were investigated. Logically, (D)-(−)-fructose was chosen as a trigger for (i) its highest binding constant with PBA and (ii) strongest swelling amplitude.[29]

[a] CNRS, Université de Bordeaux, Bordeaux INP, CBMN, UMR 5248, 33607, Pessac, France.
[b] Department of Applied Chemistry and Biochemistry, Kumamoto University, 2-39-1 Kurokami, Chuo-ku, Kumamoto 860-8555, Japan.
[c] Graduate School of Energy Science 3, Kyoto University, Yoshida-honmachi, Sakyo-ku, Kyoto 606-8501 Japan.
[d] Univ. Bordeaux, CNRS, Bordeaux INP, ISM, UMR 5255, F-33400 Talence, France.
[e] Department of Organic Chemistry, University of Geneva, Quai Ernest Ansermet 30, 1211 Geneva 4, Switzerland.
[f] Dipartimento di Chimica e Chimica Industriale, Università di Pisa Via Moruzzi 13, 56124 PISA, Italy.
[g] Kumamoto Industrial Research Institute, Materials Development Department, Kumamoto, JP 862-0901
[h] WPI-Advanced Institute for Materials Research, Tohoku University, Katahira, Aoba-Ku, 980-8577 Sendai, Japan

†Electronic supplementary information (ESI) available: Sample preparation method, synthetic procedures and spectral data. See DOI: 10.1039/x0xx00000x

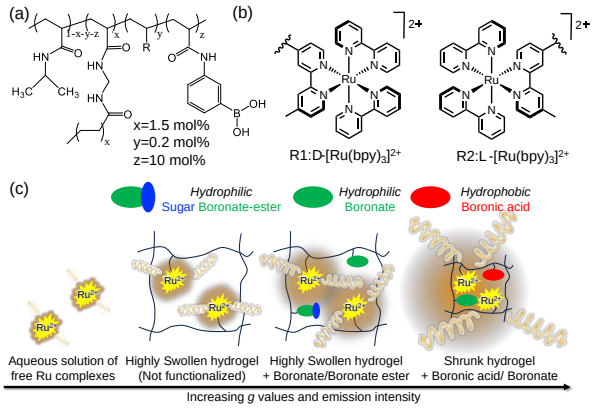

Fig. 1 (a) Structural formula of the pNIPAM-Ru-PBA microgel (R is a methyl); (b) Enantiomers of $[Ru(bpy)_3]^{2+}$ incorporated in microgels (c) Schematic representation of sugar-induced CPL switching system.

The aqueous suspension of microgels (1 ml) was mixed with phosphate buffer (1.5 ml, pH 8.5), and the hydrodynamic diameters d_H of these microgels were evaluated with dynamic light scattering (Table S1). The swelling ratio, defined as the cubic ratio of the microgel hydrodynamic diameters d_H with respect to the most shrunk microgel, can be directly inferred by comparing the hydrodynamic diameters. The PBA-microgel derivatives swell to more than double in diameter (from 122 to 263 nm) upon adding fructose. On the contrary, the d_H of microgels without PBA is about 161 nm and does not depend on the presence/absence of fructose. Of note, the $[Ru(bpy)_3]^{2+}$ functionalised microgels, with and without PBA, have roughly the same d_H in the collapsed state (respectively 88 and 80 nm), which is governed by the precipitation polymerization conditions. These control experiments demonstrated that the enantiopure $[Ru(bpy)_3]^{2+}$ grafted microgels had identical structures to the racemic one.[27,30]

Then, the study focused on the different optical properties of the microgels (UV-Vis, CD, PL and CPL), at various swelling states. These properties were first measured at 15 °C upon stirring. Microgels with and without PBA were compared to distinguish the effect of the matrix itself and the related change of polarity associated with the swelling changes, from that of the PBA-luminophore proximity, which is also triggered by the swelling. In Fig. 2 is shown the effect of the addition of fructose on the chiroptical properties of microgel of Δ-$[Ru(bpy)_3]^{2+}$ with and without PBA, noted hereafter as pNIPAM–Δ-Ru-PBA and pNIPAM–Δ-Ru, respectively. It was clearly observed that in the absence of PBA, no detectable effect was observed upon addition of fructose. On the other hand, in the presence of PBA, the impact of the fructose addition was visible both from the PL and CPL intensities as shown in Fig. 2 (c), and decreased by about a half. By contrast, only minor variations were observed for the UV-Vis and CD signals. The dissymmetry factors (g_{abs} and g_{lum}) were evaluated and shown in Tables 1 and 2. As these values are normalized either by the absorbance or the PL, one cannot simply attribute these variations to the increase of the local concentration of $[Ru(bpy)_3]^{2+}$ upon gel swelling/shrinking.

In the absence of PBA, g_{abs} for pNIPAM–Δ-Ru were 2.21 ± 0.04 × 10^{-3} (w/o fructose) and 2.20 ± 0.04 × 10^{-3} (W fructose) at 420 nm showing no effect of fructose (Fig. S1). In the presence of PBA (pNIPAM–Δ-Ru-PBA), g_{abs} shows a slight decrease upon the addition of fructose, i.e. from 2.50 ± 0.05 × 10^{-3} (w/o fructose) to 2.30 ± 0.04 × 10^{-3} (w/ fructose) at 420 nm (Fig. S2).

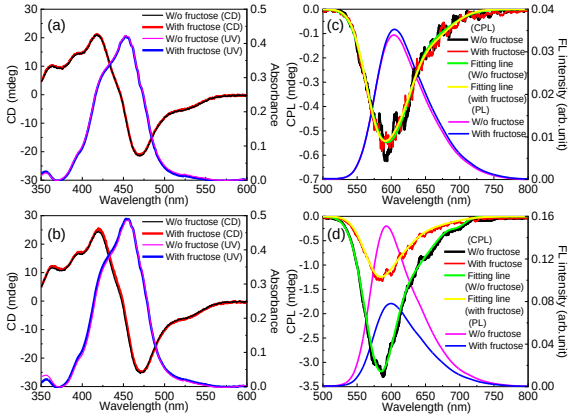

Fig. 2 CD, UV-Vis, CPL and PL spectra of microgel with and w/o PBA. (a) CD and UV-Vis spectra of pNIPAM-Δ-Ru, (b) CD and UV-Vis spectra of pNIPAM-Δ-Ru-PBA, (c) CPL and PL spectra of pNIPAM-Δ-Ru, (d) CPL and PL spectra of pNIPAM-Δ-Ru-PBA. The red and black on CD and CPL lines are the spectra with (w/) and without (w/o) fructose, respectively. The blue and purple on UV-vis and PL lines are the spectra with and w/o fructose, respectively. The UV-Vis spectrum was obtained by subtracting the baseline coming from the background spectrum of pNIPAM (owing to the light scattering by colloidal particles). Yellow and green lines are the fitting line of CPL spectra with and w/o fructose, respectively. Measurement temperature was 15 °C. Excitation wavelength of PL and CPL spectra was 420 nm. The use of (L)-(+)-fructose showed no detectable modification for the CPL data (Fig. S3).

The PL intensity in the system with PBA also decreased upon the addition of fructose which is in agreement with a previous report[28], i.e. the formation of a more hydrophilic ester between the PBA and fructose modifies the interactions between PBA moieties and ruthenium complexes. In fact, there is a cooperative effect between π-π interactions, between the phenyl rings of the boronic acid and bipyridyl groups of the $[Ru(bpy)_3]^{2+}$, and the electrostatic interaction between anionic boronate and cationic $[Ru(bpy)_3]^{2+}$ moieties. At the operating pH of 8.5, which is close to (or slightly above) the pKa of PBA without fructose as determined by the zeta potential of the microgels,[27,30] there is a coexistence between the fraction of boronic acid units, ~~and boronate are equivalent~~, which are neutral and hydrophobic and of boronates, which are charged and hydrophilic. The addition of fructose induces a switch of the first fraction into charged and hydrophilic states upon boronate ester formation. It also induces microgel swelling ~~due to the creation of sugar boronate ester~~, which increases the distance between the ruthenium complex and the PBA. ~~increases. And~~ Consequently, the emission of $[Ru(bpy)_3]^{2+}$ decreases as it induces the enhancement of non-radiative components in $[Ru(bpy)_3]^{2+}$ relaxation process[27].
Of note, the selected composition was the one which gave the best enhancement. Decreasing the PBA/$[Ru(bpy)_3]^{2+}$ was found to reduce the influence of the quantum yield and the luminescence lifetime[27].

We then investigated the variation of the dissymmetry factor of CPL, g_{lum}, of pNIPAM–Δ-Ru-PBA during the swelling. Without PBA, the g_{lum} values of pNIPAM–Δ-Ru with and without fructose were not significantly different, 1.17 ± 0.02 × 10^{-3}, 1.20 ± 0.01 × 10^{-3}, respectively. On the contrary, in the presence of PBA, the g_{lum} values clearly decreased with fructose from 1.55 ± 0.02 × 10^{-3} to 1.28 ± 0.03 x 10^{-3} (pNIPAM–

Δ-Ru-PBA) and from 1.53 ± 0.02 × 10^{-3} to 1.39 ± 0.03 x 10^{-3} (pNIPAM–Λ-Ru-PBA) along with the microgel swelling (Fig. S4).

In summary, both g_{abs} and g_{lum} are the highest for the microgels of pNIPAM–Δ orΛ-Ru-PBA without fructose. Both *g*-factors decreased upon the addition of fructose and the resulting swelling of the microgel (about ten times in volume). In the absence of PBA, no effect was observed for g_{abs} and g_{lum} with the addition of fructose, and both are smaller than that of

Table 1 Summary of g_{abs} on microgel including Δ-ruthenium complex

g_{abs} (x 10^{-3})	w/o PBA	w/ PBA
w/o fructose	2.21 ± 0.04	2.50 ± 0.05
w/ Fructose	2.20 ± 0.04	2.30 ± 0.04

Table 2 Summary of g_{lum} on microgel including ruthenium complex

g_{lum} (x 10^{-3})	w/o PBA	w/ PBA
w/o fructose	Δ[a]: 1.17 ± 0.05	Δ: 1.55 ± 0.02 Λ[b]: 1.53 ± 0.02
w/ Fructose	Δ: 1.17 ± 0.03	Δ: 1.28 ± 0.03 Λ: 1.39 ± 0.03

g_{abs} (= *θ(mdeg)/A*32981*) was evaluated at 420 nm (chosen as the excitation wavelength) and g_{lum} (= 2Δ*I (λ)/I(λ)*) was evaluated at the peak top in the CPL spectrum. [a] Microgel including Δ-Ru. [b] Microgel including Λ-Ru. The error is calculated by the standard deviation of the fitting curve[†ESI].

the microgels with PBA. Indeed, in all cases (with or without fructose), g_{abs} and g_{lum} are higher in the presence of PBA.

It has been reported that the *g* values are closely correlated to the mobility of $[Ru(bpy)_3]^{2+}$ [12,13]. In the present case, the increasing *g* values for the shrunk microgels can originate from two possible mechanisms. First, the mobility of $[Ru(bpy)_3]^{2+}$ derivatives in pNIPAM-Ru-PBA is locally restricted by the strong interaction with PBA. The other reason for the decreasing mobility of $[Ru(bpy)_3]^{2+}$ derivatives can be related to the global rigidification of the collapsed microgel network.

As seen in Table 1 and 2, the *g*-factors of the swollen gels with PBA and fructose are still slightly higher than those without PBA (with or without fructose) although the former are larger (263 nm diameter) than the latter (161 nm diameter). This indicates that the swelling ratio is not the main determining factor for the *g* values but other local environment of $[Ru(bpy)_3]^{2+}$ should be taken into account.

We therefore investigated the effect of the particle sizes of the microgel on their g_{lum} while varying the temperature. In Figure 3, the variations of particle size and g_{lum} are shown for the microgels (a) w/o PBA w/o fructose, (b) w/ PBA w/ fructose, and (c) w/o PBA w/o fructose, respectively. It should be reminded that the microgel collapsing temperature is related to the hydrophobicity of the polymer structure.

Regarding the microgels w/o PBA, although the particle sizes do decrease upon increasing temperature, no increase in g_{lum} values is observed even with the smaller particle sizes (Fig. 3(a)). This confirms that the g_{lum} values are not solely related to the swollen state of the microgel.

In the presence of PBA w/o fructose, as shown in Fig. 3(b), the particle size decreases with increasing temperature, and the corresponding g_{lum} further increases. Because the microgels flocculated at a temperature slightly above 20 °C, we did not explore higher temperatures. For the microgels w/ PBA w/ fructose (Fig. 3(c)), the presence of fructose increases the volume phase transition temperature, due to hydrophilicity increase. Above the transition temperature, highly pronounced shrinkage of the microgels is observed (260 nm @10-20 °C to 88 nm @ 40 °C), which is again accompanied by the increase of g_{lum}. Fig. 3(d) shows the temperature dependence of each sample's wavelength of PL peak. This parameter is directly related to the environment of the $[Ru(bpy)_3]^{2+}$. A blue shift indicates a more hydrophobic environment and interaction with the PBA groups, whereas a red shift indicates a more hydrophilic environment [27]. Without PBA, the peak position (blue triangle) remains almost constant at around 605 nm, regardless of the temperature. When PBA is present in the microgel, w/o fructose, the PL peak

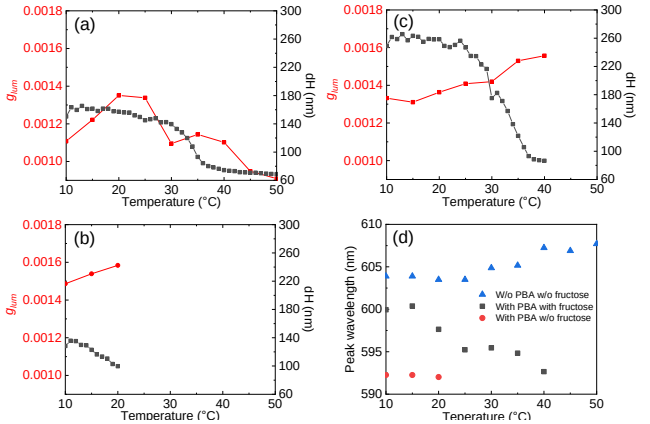

Fig. 3 Temperature dependence of g_{lum} and the particle size of microgel. (a) the microgel w/o PBA w/o fructose, (b) the microgel w/ PBA w/o fructose*, (c) the microgel w/ PBA w/ fructose, (d) temperature dependence of peak wavelength in PL spectra on each sample. *A microgel of Λ-$[Ru(bpy)_3]^{2+}$ was used.

is at around 592 nm at 10-15 °C (red circle). In the presence of fructose (black square), PL peak moves to ~600 nm at low temperature indicating the hydrophilicity of the boronate ester and its influence on the $[Ru(bpy)_3]^{2+}$. In contrast at 40 °C, it decreases to around 590 nm, identical to the value without fructose, indicating that the fructose is no more bound to the PBA group because of the shrinkage of the microgels[27]. Thus, at high temperature, the interaction between $[Ru(bpy)_3]^{2+}$ and PBA is reinforced[27]. The g_{lum} in the presence of fructose follows the evolution of the interaction between the PBA and the $[Ru(bpy)_3]^{2+}$ with temperature variation. It evolves from a value close to that of the microgels w/o PBA, corresponding to the most hydrophilic environment of the $[Ru(bpy)_3]^{2+}$, to a value close to the PBA microgels w/o fructose, corresponding to the most hydrophobic environment. From these results, the intermolecular interaction between PBA and $[Ru(bpy)_3]^{2+}$ seems to play the key role on the corresponding value of g_{lum}.

It was previously reported that the values of g_{abs} and g_{lum} are higher and closer to each other for rigid molecules with lower mobility or vibrationally restricted condition such as cyclophanes or helicenes[12,13,32,33]. In Figure 4, both g_{abs} (black columns) and g_{lum} (green columns), as well as the ratio of the two, g_{lum}/g_{abs} (red line) are plotted for the four microgel samples as well as for the molecular solution of Δ-$[Ru(bpy)_3]^{2+}$ in acetone. An excellent correlation between the *g* values and g_{lum}/g_{abs} ratio are observed. Both increased from those for the molecular solution of Δ-$[Ru(bpy)_3]^{2+}$ to the microgel w/ PBA w/o fructose. The emission lifetime of rigid molecules with lower mobility or vibrationally restricted condition is longer than that of flexible molecules with high mobility[27]. Therefore, the longer emission lifetime from a microgel means the $[Ru(bpy)_3]^{2+}$ has the lower mobility[27]. PL lifetime of each microgel shows the same tendency with both g_{abs} and g_{lum} as demonstrated in Fig. 4 (blue columns). This indicates that the g_{lum} and g_{abs} correlate with the rigidity of the microgel by the

effect of PBA and fructose. As we have previously reported, the rigidity of the microgels, the PL lifetime and their quantum yield (QY) are strongly correlated[27]. Therefore, we conclude that the chiroptical properties (CD and CPL intensities and their corresponding dissymmetry factors g_{lum} and g_{abs}) of these microgels are strongly enhanced when their rigidity is higher[27] (with longer PL lifetime and higher QY).

In conclusion, we investigated the optical properties, UV-vis, PL,
CD and CPL, of pNIPAM microgels functionalized by enantiopure

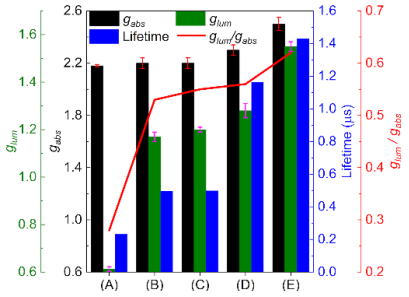

Fig. 4 Comparison of g_{lum}, g_{abs}, PL lifetime* and g_{lum}/g_{abs} of $[Ru(bpy)_3]^{2+}$ on microgels at 15 °C. (A) Δ-Ru-$(bpy)_3$ in acetone solution, (B) pNIPAM–Δ-Ru w/ fructose, (C) pNIPAM–Δ-Ru w/o fructose, (D) pNIPAM–Δ-Ru-PBA w/ fructose, (E) pNIPAM–Δ-Ru-PBA w/o fructose. Yellow bar is g_{abs}, green bar is g_{lum}, and red line is g_{lum}/g_{abs}. *PL lifetime was measured at 25 °C by 405 nm excitation wavelength.

$[Ru(bpy)_3]^{2+}$ with PBA as a luminescence enhancer. Both g_{abs} and g_{lum} as well as their ratio are clearly higher in microgels than in free solution of $[Ru(bpy)_3]^{2+}$ derivatives and these values are further enhanced when the interaction between the $[Ru(bpy)_3]^{2+}$ and PBA grafted pNIPAM microgels increases upon gel shrinking and consequently the molecular mobility of $[Ru(bpy)_3]^{2+}$ is suppressed. This was demonstrated by using internal triggers such as fructose and temperature that serve to modulate the interaction between PBA and $[Ru(bpy)_3]^{2+}$. Such mechanisms have never been reported for the modulation of chiroptical signals and could be extended to other classes of responsive polymers conjugated with enantiopure luminophores, whose luminescent properties are controllable upon swelling *via* polarity modulation,[34] or variation of the donor-acceptor distance exhibiting the Förster resonance energy transfer.[35,36] Such a use of PL and chiroptical techniques to obtain micro-chiral-environment information within microgels represents a promising approach for the development of a new generation of tunable CPL optical devices and a new class of luminescent colloidal sensors.

Conflicts of interest

There are no conflicts to declare.

Acknowledgements

K.Y, Y.O and R.O thank JSPS Overseas Research Fellowships, CNRS and Bordeaux University in the context of LIA-CNPA. F.Z. and J. L. thank the University of Geneva for financial support.

Notes and references

1 D.-W. Zhang, M. Li and C.-F. Chen, *Chem. Soc. Rev.*, 2020, **49**, 1331–1343.
2 Y. Wang, M. Li, J. Teng, H. Zhou, W. Zhao and C. Chen, *Angew. Chem.*, 2021, **133**, 23811–23816.
3 F. Zinna, L. Arrico, T. Funaioli, L. Di Bari, M. Pasini, C. Botta and U. Giovanella, *J. Mater. Chem. C*, 2022, **10**, 463–468.
4 L. Wan, X. Shi, J. Wade, A. J. Campbell and M. J. Fuchter, *Advanced Optical Materials*, 2021, **9**, 2100066.
5 K. Dhbaibi, L. Abella, S. Meunier-Della-Gatta, T. Roisnel, N. Vanthuyne, B. Jamoussi, G. Pieters, B. Racine, E. Quesnel, J. Autschbach, J. Crassous and L. Favereau, *Chem. Sci.*, 2021, **12**, 5522–5533.
6 C. Wang, H. Fei, Y. Qiu, Y. Yang, Z. Wei, Y. Tian, Y. Chen and Y. Zhao, *Appl. Phys. Lett.*, 1999, **74**, 19–21.
7 J. Yuasa, T. Ohno, H. Tsumatori, R. Shiba, H. Kamikubo, M. Kataoka, Y. Hasegawa and T. Kawai, *Chem. Commun.*, 2013, **49**, 4604.
8 Y. Imai, Y. Nakano, T. Kawai and J. Yuasa, *Angew. Chem. Int. Ed.*, 2018, **57**, 8973–8978.
9 P. Stachelek, L. MacKenzie, D. Parker and R. Pal, *Nat Commun*, 2022, **13**, 553.
10 Y. Sang, J. Han, T. Zhao, P. Duan and M. Liu, *Adv. Mater.*, 2020, **32**, 1900110.
11 L. E. MacKenzie and R. Pal, *Nat Rev Chem*, 2021, **5**, 109–124.
12 H. Tanaka, Y. Inoue and T. Mori, *ChemPhotoChem*, 2018, **2**, 386–402.
13 N. Chen and B. Yan, *Molecules*, 2018, **23**, 3376.
14 E. M. Sánchez-Carnerero, A. R. Agarrabeitia, F. Moreno, B. L. Maroto, G. Muller, M. J. Ortiz and S. de la Moya, *Chem. Eur. J.*, 2015, **21**, 13488–13500.
15 L. Arrico, L. Di Bari and F. Zinna, *Chem. Eur. J.*, 2021, **27**, 2920–2934.
16 G. Albano, G. Pescitelli and L. Di Bari, *Chem. Rev.*, 2020, **120**, 10145–10243.
17 T. Goto, Y. Okazaki, M. Ueki, Y. Kuwahara, M. Takafuji, R. Oda and H. Ihara, *Angew. Chem. Int. Ed.*, 2017, **56**, 2989–2993.
18 T. Harada, H. Yanagita, N. Ryu, Y. Okazaki, Y. Kuwahara, M. Takafuji, S. Nagaoka, H. Ihara and R. Oda, *Chem. Commun.*, 2021, **57**, 4392–4395.
19 N. Shi, J. Tan, X. Wan, Y. Guan and J. Zhang, *Chem. Commun.*, 2017, **53**, 4390–4393.
20 A. Homberg, E. Brun, F. Zinna, S. Pascal, M. Górecki, L. Monnier, C. Besnard, G. Pescitelli, L. Di Bari and J. Lacour, *Chem. Sci.*, 2018, **9**, 7043–7052.
21 N. Saleh, B. Moore, M. Srebro, N. Vanthuyne, L. Toupet, J. A. G. Williams, C. Roussel, K. K. Deol, G. Muller, J. Autschbach and J. Crassous, *Chem. Eur. J.*, 2015, **21**, 1673–1681.
22 K. Dhbaibi, L. Favereau, M. Srebro-Hooper, C. Quinton, N. Vanthuyne, L. Arrico, T. Roisnel, B. Jamoussi, C. Poriel, C. Cabanetos, J. Autschbach and J. Crassous, *Chem. Sci.*, 2020, **11**, 567–576.
23 Y. Hashimoto, T. Nakashima, D. Shimizu and T. Kawai, *Chem. Commun.*, 2016, **52**, 5171–5174.
24 F. Song, Y. Cheng, Q. Liu, Z. Qiu, J. W. Y. Lam, L. Lin, F. Yang and B. Z. Tang, *Mater. Chem. Front.*, 2019, **3**, 1768–1778.
25 Y. Guo, Y. Han and C.-F. Chen, *Front. Chem.*, 2019, **7**, 543.
26 M. Louis, R. Sethy, J. Kumar, S. Katao, R. Guillot, T. Nakashima, C. Allain, T. Kawai and R. Métivier, *Chem. Sci.*, 2019, **10**, 843–847.
27 S. A. Denisov, F. Pinaud, M. Chambaud, V. Lapeyre, B. Catargi, N. Sojic, N. D. McClenaghan and V. Ravaine, *Phys. Chem. Chem. Phys.*, 2016, **18**, 16812–16821.
28 J. P. Lorand, J. O. Edwards, *J. Org. Chem.*, 1959, **24**, 769–774.
29 G. Springsteen and B. Wang, *Tetrahedron*, 2002, **58**, 5291-5300.
30 M.-C. Tatry, Y. Qiu, V. Lapeyre, P. Garrigue, V. Schmitt, V. Ravaine, *J. Colloid Interface Sci.*, 2020, **561**, 481-493.
31 M. Oppermann, B. Bauer, T. Rossi, F. Zinna, J. Helbing, J. Lacour and M. Chergui, *Optica*, 2019, **6**, 56-59 and references therein.
32 M. Cei, L. Di Bari, F. Zinna, *Chirality*, 2023, **35**, 192-210
33 J. L. Greenfield, J. Wade, J. R. Brandt, X. Shi, T. J. Penfold and M. J. Fuchter, *Chem. Sci.*, 2021, **12**, 8589–8602.

34 K. Okabe, N. Inada, C. Gota, Y. Harada, T. Funatsu and S. Uchiyama, *Nat. Commun.*, 2012, **3**, 705-713.
35 D. Wang, T. Liu, J. Yin and S. Liu, *Macromolecules*, 2011, **44**, 2282–2290.
36 F. Pinaud, R. Millereux, P. Vialar-Trarieux, B. Catargi, S. Pinet, I. Gosse, N. Sojic and V. Ravaine, *J. Phys. Chem. B*, 2015, 119, **40**, 12954–12961.